

The application of the composite porous materials to reduce the harmful compounds in mainstream smoke

Yi Cao¹, Ming Bo Yue¹, Jing Yang¹, Ting Ting Zhuang¹, and Jian Hua Zhu^{1*}

Mariana Ghosh², Jasper Van Heemst², and Fiona Cunningham²

1. Key Laboratory of Mesoscopic Chemistry of MOE, School of Chemistry and Chemical Engineering, Nanjing University, Nanjing 210093, China (Fax: 0086-25-83317761; Tel: 0086-25-83595848; E-mail: jhzhu@netra.nju.edu.cn)
2. British American Tobacco, Group R&D Centre, Southampton, SO15 8TL. U.K.

Abstract: In order to reduce the harmful compounds in cigarette smoke, two types of composite porous materials are synthesized. Based on mesoporous materials, SBA-15 and MCM-41, zeolites HZSM-5 and NaY fragments are introduced into the synthetic system and assembled with mesoporous materials. These composite porous materials combine the advantages of micro- and mesoporous materials. And they exhibit higher effects on reducing the tar free radicals, TSNAs and some vapor phase compounds than activated carbon. In another way, zeolite HZSM-5 is coated into activated carbon and tailored by alkali solution, respectively. Their ability on reducing TSNAs in mainstream smoke is also obviously improved compared with activated carbon.

Keywords: zeolite; mesoporous material; activated carbon; composite porous material; mainstream smoke; carcinogenic compound

1. INTRODUCTION

Tobacco and tobacco products are widely consumed in the world. It is reported that there are 350 million people in China and 2.02 trillion sticks of cigarettes produced in 2006 [1]. Therefore, the remarkable economic benefit of tobacco industry brought to a country cannot be ignored. However, the pollution and health hazard caused by smoking have been a serious problem to the world. In 1996, scientists Green and Rodgman reported that tobacco smoke contains more than 4800 components [2]. With the development of chemical analytical techniques and the increase knowledge of genotoxic environmental agents, 69 carcinogens were identified in tobacco smoke, and several were tumor promoters or cocarcinogens. The major toxic agents are nicotine, carbon monoxide, hydrogen cyanide, nitrogen oxides, some volatile aldehydes, some alkenes, and some aromatic hydrocarbons. Therefore, it is imperative to reduce the harmful components in cigarette smoke to protect the health of human.

As a common consensus, cigarette smoke is composed of a vapor phase and the particulate phase. The vapor phase can be considered as a mixture of the smoke aerosol that can pass through the Cambridge glass filter. The particulate phase is composed of a lot of semi- and non-volatile compounds, and the particle sizes range from 0.1 to 1.0 μm in diameter. Therefore, the glass fiber filter can trap the particulate phase. Normally, the carcinogenic and toxic compounds, such as carbon oxide, volatile alkenes, and volatile *N*-nitrosamines etc. are existed in the vapor phase. Nicotine, tobacco specified *N*-nitrosamines (TSNAs), nonvolatile hydrocarbons, and polynuclear aromatic hydrocarbons (PAHs) etc. are the part constituents of the particulate matter in the mainstream smoke. In addition, some compounds can be found in both of the vapor phase and the particulate phase. For example, some semi-volatile agents, such as phenol, appear to some extent in the vapor phase. Moreover, some semi-volatile *N*-nitrosamines and volatile compounds can also be detected in the particulate phase as the aerosol type. Altogether, the existence status of these carcinogenic and toxic compounds in cigarette smoke is very complicated.

In order to protect the human from the health risk caused by cigarette smoke, it is necessary to take some methods to control the negative influence of cigarette smoke effectively and decrease the concentration of the harmful compounds in it. Although some carcinogenic compounds, such as TSNAs, are formed during curing and aging process of tobacco, most of these compounds were regenerate by the pyrosynthesis in the burning cone and the hot zones of the cigarette. Therefore, these are two main methods to add additives to reduce the

carcinogenic compounds in mainstream smoke. One-way is to mix the additives, such as zeolite NaY [3], with tobacco fibers directly and activate them when the hot zone in burning cigarette approaches them. Though the additives are always innocuous and stable under high temperature, the mixing process is inconvenient. And because the additives will participate in the burning process, it will change and bring uncertain factors to the burning routine. The other method, which is widely used, is to add the additives into the cigarette filter tips. Usually, activated carbon is selected as the filter additive though it cannot selectively adsorb carcinogenic component such as nitrosamines [4, 5]. Zeolite is another kind of additive that exhibits selectively adsorptive ability to reduce the amount of carcinogens in smoke [6]. Zeolite NaY can even trap 85% of *N*-nitrosopyrrolidine (NPYR) at 453 K when NPYR passed through it [7]. However, due to the limitation of micropore size, zeolites fail to trap bulky nitrosamines such as TSNAs. On the contrary, mesoporous material, such as SBA-15, has a higher activity than zeolite NaY for degrading bulky TSNAs such as *N*-nitrosornicotine (NNN), but less active for adsorbing volatile *N*-nitrosamine (VNA) [8]. In order to overcome the inherent weakness of micro- and mesoporous materials, and combine their advantages, the concept of synthesizing the composite porous materials is naturally considered.

In this paper, zeolites fragments are introduced in the synthetic system of mesoporous materials. After surviving from the solution, these zeolite fragments are combined with the framework of mesoporous material. In order to evaluate the performance of the newly synthesized composite porous materials, volatile *N*-nitrosamines with different molecule diameter are selected for gaseous adsorption. And they are also used as the filter additives to reduce the carcinogenic compounds in mainstream smoke. For the purpose of comparison, HZSM-5 coated activated carbon along with alkali solution tailored HZSM-5 is also considered.

2. EXPERIMENTAL

2.1 Reagents and Sample Synthesis

N-nitrosodimethylamine (NDMA), *N*-nitrosopyrrolidine (NPYR) and *N*-nitrosohexamethyleneimine (NHMI) were purchased from Sigma and dissolved in dichloromethane in a volume ratio of 1:19. Zeolite NaY and HZSM-5 (Si/Al=12.5) were commercially available powders, and all reagents used were of AR grade. The cigarette used in this paper is Virginia type signed as X148.

The composite porous material named SZ was prepared using tetraethyl orthosilicate (TEOS) and HZSM-5 (Si/Al=12.5) as silica and ZSM-5 precursors, respectively. About 2.0 g Pluronic

P123 (ethylene oxide (EO)/ propylene oxide (PO) triblock copolymer, composition EO₂₀PO₇₀EO₂₀, Aldrich) was mixed with 60 g 2M HCl, 15 g H₂O in a beaker and stirred at room temperature. When the solution turned to clear, 1.2 g HZSM-5 was added into the solution, and stirred this solution for 3 h at 313 K. Adding 4.25 g TEOS into the solution and stirred for another 24 h at 313 K. The synthesized gels were autoclaved at 373 K for 24 h. As-made solid material was filtered, washed several times and air-dried. The resultant powder was calcined in a flow of air for 6 h at 823 K with the flow rate of 500 ml/min to remove the template.

About 3 g SiO₂ (100 mesh) was dissolved in 45 ml 0.56 M NaOH solution as the silicic precursor at 333 K. And then, 3 g NaY was added into this solution and stirred for 2 h. This solution was labeled as solution A. Solution B was the aqueous solution of CTAB that dissolved about 4.55 g CTAB in 25 g H₂O. And then, the solution B was dropped into the solution A slowly with continuous stirring. After dropping the solution, the pH value of this mixture was adjusted to 11 by using 2 M HCl. The solution was stirred for another 6 h, and removed to an autoclave at 373 K for 72 h. As-made solid material was filtered, washed and dried at room temperature. The resultant powder was calcined in a flow of air for 5 h at 823 K with the flow rate of 500 ml/min.

3.6 g activated carbon (coconut shell based carbon) was mixed with 1.53 g TEOS by using 7 ml ethanol. This mixture was stirred and dried at 323 K. 2.73 g TPAOH and 0.0731 g NaAlO₂ were mixed by using 4 mL ethanol, and dropped this solution slowly onto the activated carbon mentioned above. The mixture turned into the gel by continuously stirring at 323 K, and then was removed into an autoclave at 453 K for one day. The as-made material was filtered, washed and dried at room temperature. The resultant powder was calcined in a flow of nitrogen at 823 K for 6 h.

2 g zeolite NaZSM-5 (Si/Al= 26) was added in 200 ml 0.1 mol/L NaOH solution, and stirred at 358 K for 5 h. After the solution was cooled, it was filtered and dried at 373 K for one night. The as-made sample was dealt by ion-exchange method [9] to made ZMM.

2.2 Characterization

The samples were characterized by powder X-ray diffraction recorded on an ARL XTRA diffractometer with Cu K α radiation in the 2 θ ranges from 0.5 to 8 degrees or from 5 to 70 degrees.

To get the FTIR spectrum of modified silica, compressed KBr pellets containing 3-wt% of sample were used and the spectrum was recorded on a Bruker 22 infrared spectrophotometer in 4000-400 cm⁻¹ with a resolution of 4 cm⁻¹.

The nitrogen adsorption-desorption isotherms at 77 K were measured in a Micromeritics ASAP 2020 system, and about 100mg of the sample (20-40 mesh) were evacuated at 573 K for 4 h in the degas port of the adsorption analyzer. The Brunauer-Emmett-Teller (BET) specific surface areas (S_{BET}) were calculated using adsorption data acquired at the relative pressure (P/P_0) range of 0.05-0.22 and the total pore volume determined from the amount adsorbed at a relative pressure of about 0.99. The pore size distribution (PSD) curves were calculated from the analysis of the desorption branch of the isotherm using the Barrett-Joyner-Halenda (BJH) algorithm [10].

Adsorption of NPYR was performed in a stainless steel micro-reactor with 3 mm diameter and 150 mm length. 5 mg sample (20-40 mesh) was filled in the one end of the reactor and sealed by glass wool to fix the position. And this part was inserted deeply into the injector port of Varian 3380 GC and another end connects with the separation column in the GC [11]. The sample was directly heated to 338 K in He flow with a rate of 30 ml/min, and the NPYR solution was pulse injected with

amounts of 2 μ l each time. The TCD of GC analyzed the gaseous effluent, and the decrement in the ratio of solute to solvent utilized to calculate the adsorbed amount [8].

In situ FTIR experiments were performed in a home-built IR cell with CaF₂ windows. A Bruker 22 spectrometer, with a resolution of 4 cm⁻¹, was used. The samples disc, with a density of 15 mg/cm², was activated at 773 K in N₂ flow for 2 h, and then the background spectra were collected on the activated adsorbate-free sample. 0.4 μ l NPYR was then introduced into the IR cell at 493 K and the sample was purged with nitrogen flow for 10 min to remove the physically adsorbed nitrosamines prior to recording the FTIR spectrum.

In order to reveal the effect of composite porous materials as the filter additives, 40 mg sample (20-40 mesh) was added into the middle of the X148 cigarette filter. And all the cigarettes were conditioned for at least 48 h at 22°C and 60% R.H. before testing. The effect of the porous materials to reduce the TSNAs, tar free radicals, and vapor phase components in mainstream smoke was estimated as follows.

Three cigarettes were smoked on an RM20 smoking machine under ISO conditions (35 cm³ puff, 2-s duration every 60 s) onto a Cambridge filter pad. The TSNAs on the pad were extracted by 30 ml of methanol for 30 minutes using an orbital shaker. Internal standard was added at the start of the extraction. All cigarette types were smoked in triplicate. A 2R4F sample was smoked at the start as a quality control/system suitability check.

Five cigarettes were smoked using a 20-port smoking machine (Heinrich Borgwaldt) under the ISO conditions. The particulate phase was trapped on a cellulose acetate filter rod that was then inserted directly into the ESR cavity (JEOL-FR30EX) [12, 13].

Three cigarettes were smoked by using a single-port Burgwaldt smoking machine under the ISO standard conditions. The mainstream smoke was collected by a Tedlar bag through a Teflon tube (SKC INC. USA). A set of HP 6890 GC and HP 5972 MSD was utilized to analyze and determine the compounds in the vapor phase. Peak assignments in the GC-MS chromatograms were made using an on-line library, the Wiley Registry of Mass Spectral Data, 6th Edition, by F.W. McLafferty.

3. RESULTS AND DISCUSSION

3.1 The structure properties of composite porous materials

All the XRD profiles of the porous materials are provided in Figure 1. In the low-angle region, SZ sample (Fig. 1a) exhibits three well-resolved diffraction peaks indexed to the (100), (110) and (200) reflections that are the characteristic XRD patterns of 2D-hexagonal pore ordering in the *P6mm* space group [14], closely matching to the XRD pattern of SBA-15. In the Figure 1c, there is some residual diffraction peaks of ZSM-5 zeolite remained in the high-angle XRD patterns of SZ, reflecting the survival of zeolite fragments from the strong acidic synthetic system along with the existence of microporous structure in these fragments. Owing to the insertion or blockage of the ZSM-5 zeolite fragments into the channel of SBA-15, the XRD diffraction intensity of SZ sample was slightly reduced, however, SZ sample still kept the similar mesoporous structure of SBA-15.

Figure 1b presents the XRD pattern of MNY sample. Compared with MCM-41, the XRD profile of MNY sample also shows special (100), (110) and (200) diffraction peaks. However, due to the introduction of zeolite NaY into the synthetic system, the aluminum was incorporated into the lattice of MCM-41. Therefore, the intensity of the 100 plane was lower and the 110 and 200 peaks were overlapped into a broad hump. That is to say, introduction of aluminum during the synthesis procedure decreases the ordering and brings down the structural uniformity

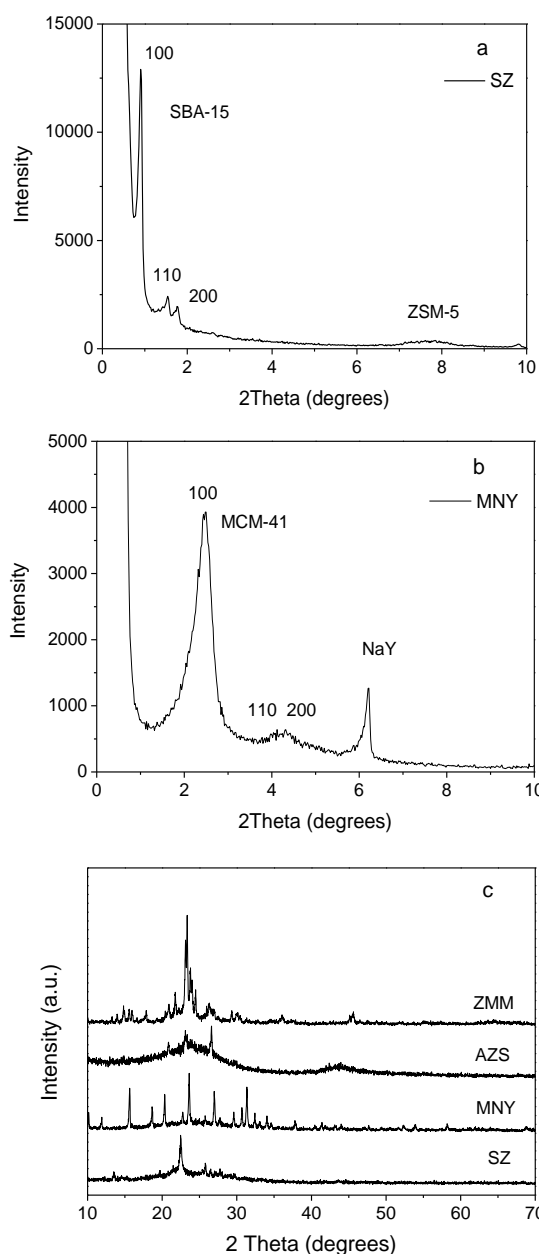


Figure 1. XRD patterns of (a) low-angle signal of SZ; (b) low-angle signal of MNY; (c) high-angle results of SZ, MNY, AZS and ZMM samples.

of MCM-41; But MNY still maintained the similar mesoporous structure with MCM-41. The high-angle XRD result shows clear XRD diffraction peaks of zeolite NaY on MNY sample, which confirms the fragments of zeolite NaY were survived partly from the alkali synthetic system. That is to say, MNY sample possesses both of mesoporous and microporous structure. However, the influence of the introduction of zeolite NaY into the synthetic step still could be seen from the XRD patterns. Firstly, the d_{100} of MNY is 2.8 nm (Table), a small shift to lower d -spacing relative to the MCM-41. Secondly, the peaks of (110) and (200) reflections of MNY overlapped into a broad hump that is different with MCM-41. These two phenomena show that the introduction of zeolite NaY will bring a little deterioration to MCM-41, which decreased its ordering and the structural uniformity more or less.

Revealed by the scanning electron micrographs (SEM) of SZ and MNY samples (Fig. 2 and Fig. 3), it is very clearly that SZ and MNY have different morphology. SZ sample has a fiberlike morphology in microcosm, and its particle size is about 2-4 μm .

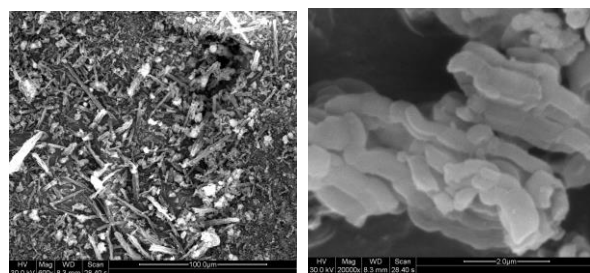


Figure 2. Scanning electron micrographs of SZ sample.

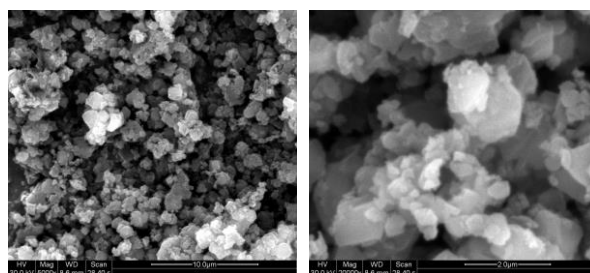


Figure 3. Scanning electron micrographs of MNY sample.

MNY sample looks like a lot of particles deposit together. And its size is also smaller than SZ sample, which is only 0.5-2 μm .

Figure 1c also provides the XRD patterns of AZS and ZMM samples. AZS sample shows two broad peaks centered at 2θ of 24° and 43° , which can be assigned to nano-sized carbon [15]. And three small diffraction peaks were appeared on the first broad peak, which could be considered as the diffraction signals of zeolite ZSM-5. After deal zeolite ZSM-5 with the NaOH solution, most ZSM-5 fragments survived from the alkali environment, and the XRD pattern showed ZMM sample maintained the crystalline structure of zeolite MFI except a little decrease on its diffraction intensity.

Figure 4a represents the N_2 adsorption-desorption isotherm of SZ sample. It is well known that SBA-15 always exhibits an isotherm with H1 type hysteresis loop at high relative pressure, while SZ sample possessed the H2 type hysteresis loop, mirroring the pore blocking effects present in it, because SZ sample comprise the open and closed cylindrical mesoporous containing some plugs [16]. Together with the high-angle XRD patterns of SZ as mentioned above, it is safe to infer that ZSM-5 fragments survived from the strong acidic synthesis, have inserted and/or blocked the cylindrical mesoporous channels to reduce the pore sizes, and moreover, these fragments may keep some microstructure of parent zeolites as characterized by XRD patterns (Fig. 1c). On the other hand, these fragments seem to be well dispersed in the mesostructure of SZ sample because only a slight hindrance of pore was detected: referring to the nitrogen adsorption, the SZ sample had a BET surface area of $545 \text{ m}^2/\text{g}$ while the average pore diameter was about 9.1 nm (Table), a little smaller than that of SBA-15 (9.3 nm). Therefore, the Al-containing SBA-15 composite with the mesoscopic order and some microstructure of the zeolite is obtained as expected.

Figure 4b is the N_2 adsorb-desorption isotherm of MNY sample. This curve is the typical of type IV isotherm and displays one step at about P/P_0 equals to 0.34, which is the well-known capillary condensation of MCM-41-like mesoporous material. Although the introduction of zeolite NaY fragments results in a little decrease of the surface area and porosity compared with MCM-41, zeolite NaY indeed survived from the alkali environment and successfully formed micropores in the mesoporous material. Moreover, the existence of the significant hysteresis loop in the isotherm indicates that

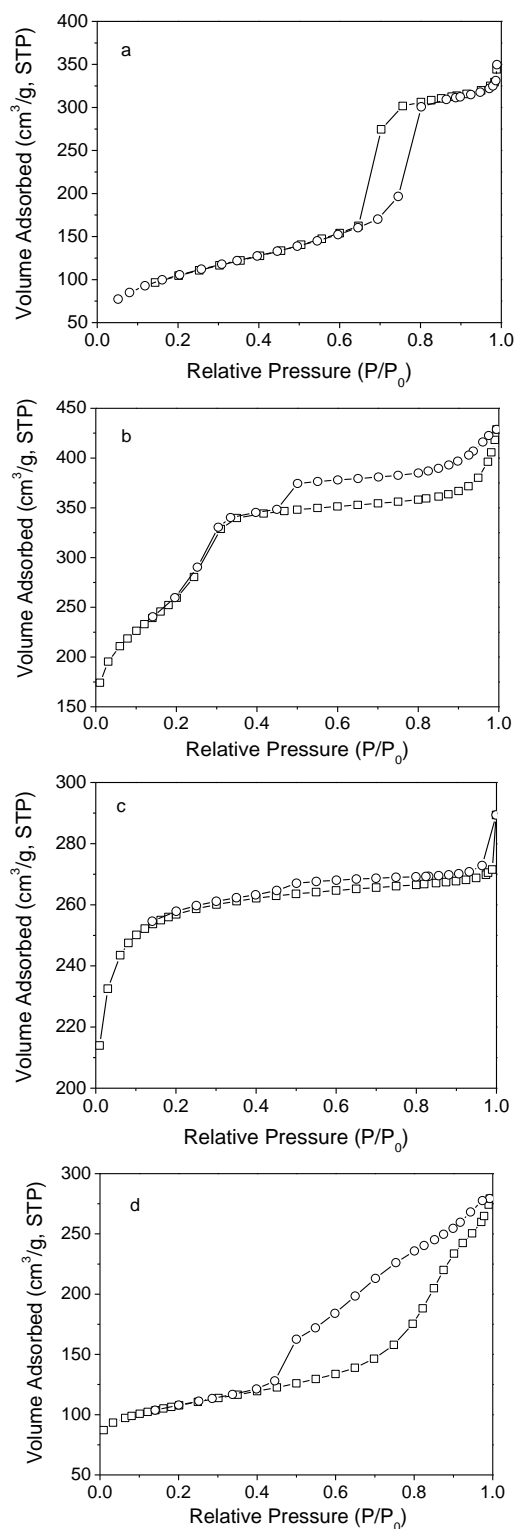


Figure 4. Adsorption-desorption isotherms of nitrogen at 77 K for (a) SZ; (b) MNY; (c) AZS and (d) ZMM.

zeolite NaY fragments partly blocked the mesopore system.

The isotherm curve of sample AZS showed a shape close to type I but a hysteresis loop occurred at the relative pressure about 0.45, reflecting the existence of microporous and mesoporous pores in it (Figure 4c). Table 1 shows that the surface area of AZS is 867 m²/g, larger than SZ but less than MNY sample. The mesoporosity value (percentage of mesopore compared to total pore volume $V_{\text{meso}}/V_{\text{tot}}$) of the AZS sample is only 21.4%, but the microporosity value reaches to 78.6%. These data suggest that the introduction of zeolite ZSM-5 pronounced improved the number of micropores in activated

carbon.

Figure 4d reveals the N₂ adsorption-desorption isotherm curves of ZMM sample. As a zeolite, the precursor of ZMM, HZSM-5 always shows a type I isotherm curve with a small hysteresis loop, suggesting that the micropores are dominant in zeolite HZSM-5. After eroded the zeolite HZSM-5 with NaOH solution, the isotherm curve of ZMM sample changed a lot. The most obvious phenomenon is the enlargement of the hysteresis loop, which indicated the formation of mesopores. Because the corruption of HZSM-5 is a process from the outside to inside, therefore, most of the mesopores open their orifices on the out surface of ZMM sample. In addition, the volume of mesopores of ZMM sample is five times than that of zeolite HZSM-5, but the volume of micropores only decreases 20%. This is very important for improving the selective adsorption ability of the sample.

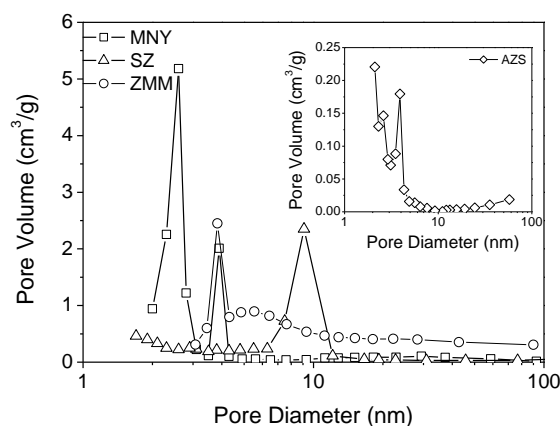


Figure 5. Pore-size distribution of the porous materials.

Table 1. Physical properties of the porous materials.

Sample	S_{BET}^a (m ² /g)	V_t^b (cm ³ /g)	V_{mic}^c (cm ³ /g)	V_{meso}^d (cm ³ /g)	D_{BJH}^e (nm)
SZ	545	0.62	0.09	0.53	9.10
MNY	916	0.61	0.05	0.56	2.68
AZS	867	0.42	0.33	0.09	1.93
ZMM	335	0.39	0.08	0.30	3.80

^a S_{BET} = BET surface area; ^b V_t = total pore volume; ^c V_{mic} = micropore volume; ^d V_{meso} = mesopore volume; ^e D_{BJH} = average pore diameter by BJH calculation.

Table 1 lists the structure parameters of all the samples, and Figure 5 shows their pore size distribution curves. Among the four modified samples, MNY sample possessed the largest specified surface area, which reached to 916 m²/g, and ZMM sample had the minimum specified surface area. After incorporated with zeolite HZSM-5 or NaY, the SZ or MNY sample obtained more micropore volume, which is helpful for the adsorption of VNA as discussed later. Similarly, ZMM sample had a close micropore volume with SZ and MNY, but its mesopore volume was less than SZ and MNY samples. The reason is the mesopore volume of ZMM was transferred from the micropores of zeolite HZSM-5 by tailoring with the alkali solution. AZS sample obtained the largest micropore volume that reached to 0.33 cm³/g, but its mesopore volume just equaled to the micropore volume of SZ sample.

Figure 6 shows the IR spectra of SZ and MNY samples in mid-IR region. SZ sample exhibits an (Si-O-Si) asymmetrical vibration band at 1090 cm⁻¹ and a symmetrical (Si-O-Si) vibration band at 806 cm⁻¹. Similar with SZ sample, MNY sample also shows these two vibration bands at 1031 cm⁻¹ and

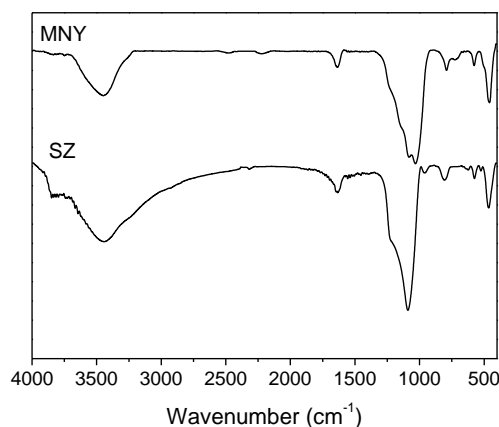


Figure 6. Infrared spectra of SZ and MNY samples.

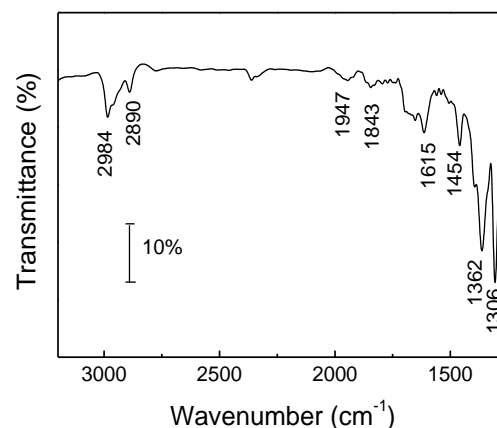
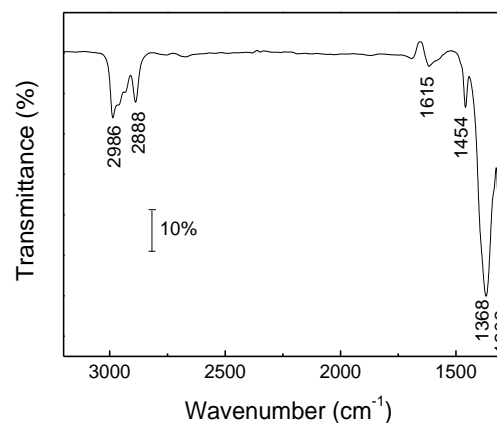
 Table 2. Adsorption of three volatile *N*-nitrosamines by SZ and MNY samples.

	NDMA		NPYR		NHMI	
	Totally injected (mmol/g)	Accumulatively adsorbed (mmol/g)	Totally injected (mmol/g)	Accumulatively adsorbed (mmol/g)	Totally injected (mmol/g)	Accumulatively adsorbed (mmol/g)
SZ	1.67	1.64	1.13	1.13	0.74	0.74
MNY	1.63	1.61	1.13	1.13	0.74	0.74

791 cm^{-1} , respectively. The band at 960 cm^{-1} of SZ sample could be assigned to the asymmetrical (Si-O) stretching mode of $\equiv\text{Si-O-H}^+$ group [17, 18], but MNY sample does not show this band. The reason should be attributed to the synthetic condition. As we know, SZ sample is synthesized from acid system, so the H^+ proton is beneficial for forming $\equiv\text{Si-O-H}^+$ group. While MNY sample is obtained from the alkali environment, which provided OH^- group for the reaction, so it is not strange for lacking the IR signal of $\equiv\text{Si-O-H}^+$ group at about 960 cm^{-1} . In addition, both of SZ and MNY samples exhibit a band at around 575 cm^{-1} , originating probably from the vibration of octahedral Al-O [19]. Being for a kind of mesoporous silica material, it is impossible to find IR signal of Al-O band in SBA-15 and MCM-41. However, by introducing the zeolite fragments into the synthetic system, such as zeolite HZSM-5 or NaY, the aluminum element was successfully introduced into these two mesoporous materials. Therefore, the IR signal of Al-O band was originated from the Al-O structure of zeolite HZSM-5 or NaY, and the newly formed Al-O band in SZ or MNY samples during the synthetic process.

3.2 Adsorption of volatile *N*-nitrosamines from gaseous phase

Table 2 shows the instantaneous adsorption of three volatile *N*-nitrosamines on SZ and MNY samples at 338 K. In this experiment, we set three specialties to reflect the adsorptive ability of samples used as the filter additives: firstly, the samples have not been thermally activated; secondly, the adsorption performs at 338 K that is closes to the temperature of cigarette filter when it is puffed; thirdly, the contact time between the nitrosamines and the samples is very short, less than 0.1 second [20]. Under the above condition, SZ and MNY samples showed the excellent adsorptive abilities to NPYR and NHMI; Both of them could trap all the NPYR or NHMI when the two nitrosamines were totally injected six times. As for NDMA, the adsorptive abilities of SZ and MNY samples have a little decrease, but still maintain the about 98% adsorptive ratio. The molecular diameter of NDMA is only $0.42 \times 0.36 \text{ nm}^2$,


 Figure 7. *In-situ* IR result of NPYR adsorbed on SZ.

 Figure 8. *In-situ* IR result of NPYR adsorbed on MNY.

smaller than NPYR ($0.42 \times 0.54 \text{ nm}^2$) and NHMI ($0.56 \times 0.53 \text{ nm}^2$) [20]. Therefore, the pore size of common mesoporous materials, such as SBA-15 and MCM-41, is too large to confine these VNAs effectively. Differently, SZ or MNY sample is the

Table 3. Smoking data of cigarette X148 and the one with additives in the filter.

Sample	NFDPM (mg/cig)	Nicotine (mg/cig)	TPM (mg/cig)	Water (mg/cig)	Puff No.	CO mg/cig
Control	10.6	0.95	13.0	1.44	7.3	9.9
Carbon	9.6	0.92	12.0	1.45	7.3	9.6
SZ	9.4	0.89	11.9	1.56	7.3	9.9
MNY	8.8	0.79	10.8	1.24	7.1	9.9

composite contains the zeolite fragments whose pore size is relatively small and fit for adsorbing VNAs. By combining the large capacity of the mesoporous materials and the effective confinement of zeolites, it is obviously that SZ or MNY samples can adsorb VNAs with a large amount. Yet it is undeniably that the adsorptive ratio of the composite mesoporous materials to VNA will decrease gradually, which seems not serious because there is not too much volatile nitrosamines in the mainstream smoke needed to be adsorbed by the filter additive.

The evidence of SZ and MNY sample adsorbs NPYR is provided by the *in-situ* FTIR experiment and shows in Figure 7 and Figure 8. In the spectrum of SZ sample, some special IR signals of NPYR appeared. The 2984 cm^{-1} and 2890 cm^{-1} bands are the ν_{as} (CH_2) and ν_{s} (CH_2) vibrations in pyrrolidinyl structure of NPYR. And the 1615, 1454 cm^{-1} bands can be considered as the ν_{as} ($\text{N}=\text{O}$) and $\nu_3(\text{NO}_2)$ vibrations in the SZ sample. The bands at 1362 cm^{-1} and 1306 cm^{-1} are considered as the signals of nitrite and vibration of C-N bond. As a kind of mesoporous silica materials, the structure of SBA-15 seems unsuitable to adsorb nitrosamines. After introducing the zeolite fragment, though the structure of the host was disturbed more or less, it is still beneficial to adsorb volatile nitrosamines. Trivalent aluminum ion may possess an attraction function for the N-NO group of volatile nitrosamines to enhance the adsorption, because the N-NO functional group of nitrosamines possesses a negative charge [21, 22]. Although the MNY sample was synthesized from alkali solution, the *in-situ* IR spectrum still shows the adsorption of NPYR on MNY sample. And the FTIR peaks are similar with that of SZ sample, indicating the adsorptive mode of MNY to NPYR is similar with SZ sample.

3.3 The application of composite porous materials as the filter additive

Table 3 provides the normal smoking data of the cigarettes which were added with the samples in the filter. Adding 40 mg of activated carbon into the cigarette filter brings a little decrease to the tar (NFDPM), nicotine, TPM and CO in the mainstream smoke, while the level of water still maintains at about 1.44 mg/cigarette. After adding SZ sample in the filter, the average puff number and the content of CO did not have any change, but the other four items had more variations than the activated carbon samples. SZ sample exhibits a little better function to remove these compounds than activated carbon, but it cannot adsorb CO from the mainstream smoke. MNY sample shows the best effect, that the reduce ratios of tar, nicotine, TPM and water are 17%, 16.8%, 16.9% and 13.9%. Why MNY sample can remove more tar, nicotine, TPM and water from MS smoke than activated carbon and SZ sample? It may originate from their different pore sizes; MNY sample possesses an average pore size with 2.68 nm while activated carbon and SZ sample have larger pore sizes.

Figure 9 shows the effect of the three materials to trap the particulate phase free radicals from the mainstream smoke. The

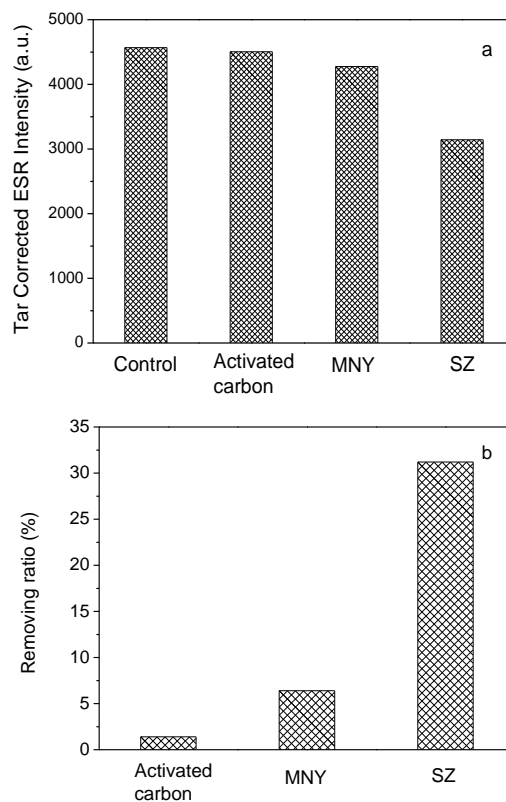


Figure 9. The results of (a) the concentration of the particulate phase free radicals and (b) removing ratios of the cigarettes with additives in the filter.

cigarettes incorporating activated carbon or MNY sample in their filters did not show an obvious function to decrease the concentration of the particulate phase free radicals, and their removing ratio was only 1.4% and 6.4%, respectively. Baum, Anderson and co-workers also analyzed the concentration of free radicals of the cigarettes with carbon filter, and found they have fairly average free radical concentration compared with the control sample [23]. That is to say, activated carbon cannot reduce the level of free radicals in mainstream smoke effectively. Differently, SZ sample exhibited very fine ability on trapping the particulate phase free radicals, and the removing ratio reached to about 31.2%. It is reported that the free radicals always existed in both gas and particulate phase [24, 25]. And the particulate phase radical of cigarette smoke has highly stable state and consist of a hydroquinone/semiquinone/quinone shuttle as found in melanins [26]. These compounds have large molecules diameter, but SZ sample has the pore size large enough for trap them. Beside, with the introduction of zeolite HZMS-5, there are many protons existed on the surface of SZ sample, which are beneficial for catching up the free radicals.

Table 4 reveals the effect of the porous materials as the filter additives to reduce the TSNAs level in the mainstream smoke.

Table 4. The results of the porous materials as the filter additives to reduce the TSNAs in the mainstream smoke

Sample	NAB		NAT		NNK		NNN	
	amount (ng/cig)	removing ratio (%)						
Control	3.18	-	26.8	-	11.1	-	14.4	-
Carbon	3.05	4.1	28.3	-5.6	10.9	1.8	15.5	-7.6
SZ	2.76	13.2	24.4	9	11.6	-4.5	12.2	15.3
MNY	2.19	31.1	19.3	28	7.97	28.2	9.98	30.7
AZS	3.04	4.4	26.5	1.1	10.1	9	13.4	6.9
ZMM	2.55	19.8	23.1	13.8	9.75	12.2	11.3	21.5

Activated carbon that is always considered as a kind of highly effective adsorbent, failed to reduce the amounts of TSNAs in mainstream smoke, i.e., the removing ratios of NAB and NNK were only 4.1% and 1.8%, and the amounts of NAT and NNN did not decrease. Incorporating HZMS-5 fragments into the pore of activated carbon slightly changed the capability, but the AZS sample still could not reduce the TSNAs obviously. None of the removing ratio was higher than 10 percent. This result may reflect that the filter additives based on activated carbon have the inherent weak ability to remove TSNAs from the mainstream smoke. However, other composite materials, which consist of silica, aluminum and oxygen, exhibited better effect than activated carbon. SZ sample could remove NNN of 15.3% and NAB of 13.2%, but its effect on NAT and NNK was still not obvious. The full improvement was firstly reflected on ZMM sample, whose removing ratios were all larger than 10 percent, and the proportion of removed NNN could reach 21.5%. MNV was the best among the five samples to reduce TSNAs level of smoke. Although the average pore size of MNV sample was smaller than SZ and ZMM samples, it had very effective but uniform function for reduction of four TSNAs, which could reduce about 28% of NAT and NNK, 30.7% of NNN and 31.1% of NAB, respectively. The molecular diameters of TSNAs are larger than VNAs. For example, NNN has a molecular size equals to $0.54 \times 0.80 \text{ nm}^2$; although this value is still smaller than the pore size of all samples we used, the results showed that the activated carbon and AZS samples, they possess the relatively small average pore sizes, have the worst effect on reducing TSNAs. With the increase of the average pore size, MNV exhibited the best reducing effect. And then, the reducing ratio decreased gradually as the pore size increasing. However, we know that TSNAs molecule do not exist alone. Most of them attach on the particulate phase whose diameter always reaches to μm grade. So it is impossible to trap these TSNAs by adsorbing them into the pore channels of composite porous materials. Up to now, it is still unclear why MNV can reduce the concentration of TSNAs in mainstream smoke. The relative reasonable explanations could be considered as the surface property and the special morphology of MNV sample. Judging from the SEM result, MNV sample looks like a lot of particles deposit together, and its particle size is 0.5-2 μm . In general, the particle sizes of the particulate phase range from 0.1 to 1.0 μm in diameter, so the size of MNV sample is more close to the particulate phase, which brings higher trapping effect to TSNAs. As the same reason, the particle size of SZ sample is about 2-4 μm , larger than that of MNV sample. Though the long fiber-like domains of SZ sample interlace each other, the spacing between these domains is still large enough for the particles of particulate phase to escape.

The results of the porous materials adsorbing the vapor phase compounds in the mainstream smoke are provided in Figure 10.

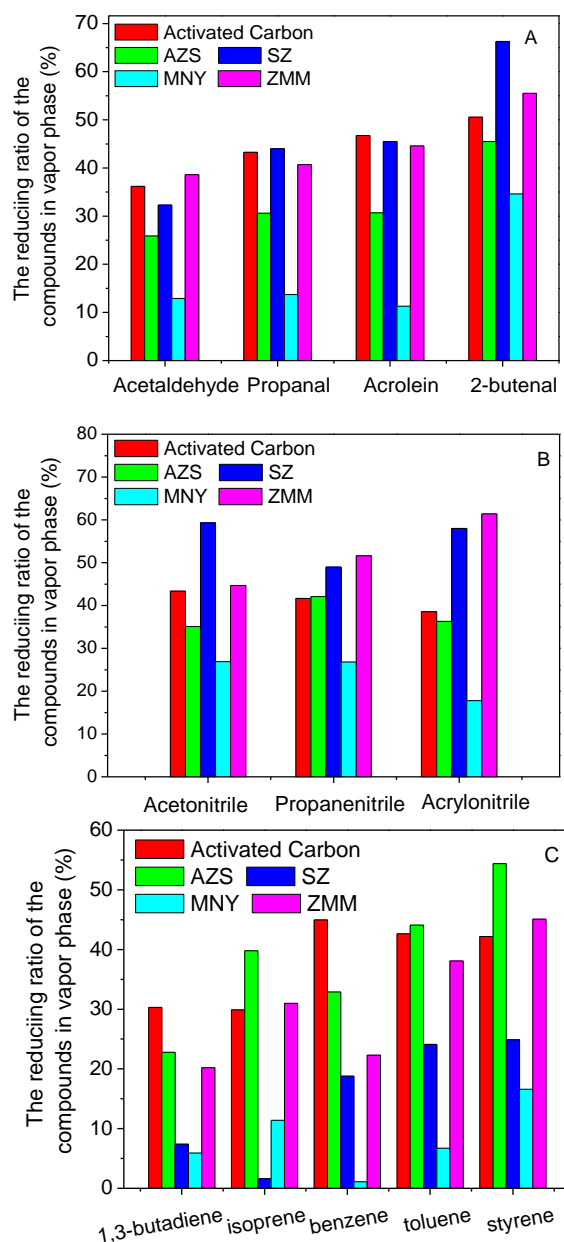


Figure 10. The effects of the porous materials to trap the vapor phase compounds as the filter additives.

The states of the substances in vapor phase are different with TSNAs, because they exist as the molecular form whose size is smaller than the pore size of the samples we used. It is very regretful to find that MNV sample did not have any advantage on removing the vapor phase compounds compared with

activated carbon. But the other three samples exhibited better effect on reducing some of compounds in the vapor phase. Modified activated carbon with HZSM-5 did not promote its adsorptive ability to aldehyde and nitrile compounds. But its adsorption capability of isoprene, toluene and styrene had been obviously improved. This result indicates that AZS sample probably fit for trap the molecules that have relative large molecule size. Among the aldehyde compounds (Figure 10a), SZ sample had higher ability in removing 2-butenal (reducing ratio is 66.3%), along with the similar reducing effect on propanal and acrolein compared with activated carbon. Only ZMM sample showed better effect on reducing acetaldehyde. As showed in Figure 10b, both SZ and ZMM samples exhibited better effect on removing nitrile compounds than activated carbon. This may reveal that SZ and ZMM samples have special affinity to the functional group of $-C\equiv CH$. In Figure 10c, SZ and ZMM samples could not reach to the reducing ratio of activated carbon. Among these compounds, toluene and styrene possess the unsaturated carbon-carbon bonds and benzene rings structure, which have relative large molecule size and high boiling point 303 K. And 1, 3-butadiene also has a large molecular size. It seems that the pore size, surface property and morphology of these mesoporous adsorbents do not take any function. Activated carbon is very effective to trap these five substances.

4. CONCLUSION

In this paper, two mesoporous silica composites named SZ and MNY were synthesized successfully. Zeolites HZSM-5 and NaY fragments can survive from the synthetic solution of SBA-15 and MCM-41, respectively, and bring less influence on their mesoporous structures. As a kind of filter additive, SZ and MNY exhibit the better ability on reducing some carcinogenic compounds in mainstream smoke than activated carbon. Activated carbon has little effect on reducing the amount of tar free radicals and TSNAs, but SZ can eliminate 31.2% of tar free radicals and MNY can trap 29.5% of TSNAs (an average reducing level) from mainstream smoke. It is revealed that composite porous materials provided in this paper has better ability on reducing the harmful compounds in mainstream smoke compared in comparison with activated carbon.

Acknowledgements Financial support from CORESTA Jury and R&D Centre of British American Tobacco in Southampton is gratefully acknowledged. And the author also would like to thank Dr. Chuan Liu for his kindly help on the experiments.

REFERENCES

- [1] T. Tuinstra, *Tobacco Report*, **2007**, *4*, 30-32.
- [2] C.R. Green and A. Rodgman, The Tobacco Chemists' Research Conference: A half-century of advances in analytical methodology of tobacco and its products. *Recent Adv. Tob. Sci.*, **1996**, *22*, 131-304.
- [3] W.M. Meier and K. Siegmann, Significant reduction of carcinogenic compounds in tobacco smoke by the use of zeolite catalyst, *Microporous and Mesoporous Mater.*, **1999**, *33*, 307-310.
- [4] D.W. Bombick, B.R. Bombick, P.A. Ayres, K. Putnam, J. Avalos, M.F. Borgerding and D.J. Doolittle, Evaluation of the genotoxic and cytotoxic potential of mainstream whole smoke and smoke condensate from a cigarette containing a novel carbon filter, *Fundam. Appl. Toxicol.*, **1997**, *39*, 11-17.
- [5] Y. Xu, J.H. Zhu, L.L. Ma, A. Ji, Y.L. Wei and X.Y. Shang, Removing nitrosamines from main-stream smoke of cigarette by zeolite. *Microporous Mesoporous Mater.*, **2003**, *60*, 125-138.
- [6] Y. Xu, Y. Wang, J.H. Zhu, L.L. Ma, L. Liu, Application of zeolite in the health science: novel additive for cigarette to remove *N*-nitrosamines in smoke. *Stud. Surf. Sci. Catal.* (Eds: R. Aiello, G. Giordano, F. Testa), **2002**, *142*, 1489-1492.
- [7] B. Shen, L.L. Ma, J.H. Zhu and Q.H. Xu, Decomposition of *N*-nitrosamines over zeolites, *Chem. Lett.*, **2000**, *4*, 380-381.
- [8] Y. Xu, Q. Jiang, Y. Cao, Y.L. Wei, Z.Y. Yun, J.H. Xu, Y. Wang, C.F. Zhou, L.Y. Shi and J.H. Zhu, The synthesis of novel porous functional materials for use as nitrosamine traps. *Adv. Funct. Mater.*, **2004**, *14*, 1113-1123.
- [9] T.F. Guiedry and G.L. Price, The conversion of 1-propanamine on copper-containing MFI and BEA zeolites prepared by aqueous and vapor ion-exchange. *J. Catal.* **1999**, *181*, 16-27.
- [10] R. Preussmann, Public health significance of environmental *N*-nitroso compounds. *WHO, IARC, Scientific Publications*, Lyon, **1983**, *45*, 3-17.
- [11] Y. Cao, L.Y. Shi, C.F. Zhou, Z.Y. Yun, Y. Wang and J.H. Zhu, Novel amorphous functional materials for trapping nitrosamines, *Environ. Sci. & Technol.* **2005**, *39*, 7254-7259.
- [12] M. Ghosh, R. Baker, C. McGrath and F. Cunningham, Investigation of free radicals in cigarette smoke by electron spin resonance: development of a quantification method. *Advanced Techniques & Applications of EPR*, the 39th Annual International meeting, University of Edinburgh, **2006**, poster 23.
- [13] M. Ghosh, F. Cunningham, R.R. Baker and J. McAughey, Development of a quantification method for free radicals in cigarette smoke by electron spin resonance. EUCHEM Conference on Organic Free Radicals, Scandinavian Collaboration for the 2006 Conference, Bergen, Norway, **2006**, poster 45.
- [14] D. Zhao, F. Feng, Q. Quo, N. Melosh, G.H. Fredrickson, B.F. Chmelka and G.D. Stucky, Triblock copolymer syntheses of mesoporous silica with periodic 50 to 300 angstrom pores. *Science*, **1998**, *279*, 548-552.
- [15] A. Manivannan, M. Chirila, N.C. Giles and M. S. Seehra, Microstructure, dangling bonds and impurities in activated carbons, *Carbon*, **1999**, *37*, 1741-1747.
- [16] B. Van Der Voort, P.I. Ravikovitch, K.P. De Jong, M. Benjelloun, E. Van Bavel, A.H. Janssen, A.V. Neimark, B.M. Weckhuysen and E.F. Vansant, A new templated ordered structure with combined micro- and mesopores and internal silica nanocapsules. *J. Phys. Chem. B*, **2002**, *106*, 5873-5877.
- [17] S.C. Laha, P. Mukherjee, S.R. Sainkar and R. Kumar, Cerium containing MCM-41-type mesoporous materials and their acidic and redox catalytic properties. *J. Catal.*, **2002**, *207*, 213-223.
- [18] K. Vidya, S.E. Dapurkar, P. Selvam, S.K. Badamali, D. Kumar and N.M. Gupta, Encapsulation, characterization and catalytic properties of uranyl ions in mesoporous molecular sieves. *J. Mol. Catal. A: Chem.*, **2002**, *181*, 91-97.
- [19] A.M. Orlovi, D.T. Janakovi, S.A. Drmani, Z. Marinkovi and D.U. Skala, Alumina/silica aerogel with zinc chloride as an alkylation catalyst. *J. Serb. Chem. Soc.*, **2001**, *66*, 685-695.
- [20] C.F. Zhou, Y. Cao, T.T. Zhuang, W. Huang and J.H. Zhu, Capturing volatile nitrosamines in gas stream by zeolites: why and how. *J. Phys. Chem. C*, **2007**, *111*, 4347-4357.
- [21] C.F. Zhou, Z.Y. Yun, Y. Xu, Y.M. Wang, J. Chen and J.H. Zhu, Adsorption and room temperature degradation

- of *N*-nitrosodiphenylamine on zeolites. *New J. Chem.*, **2004**, 28, 807-814.
- [22] Z.Y. Yun, J.H. Zhu, Y. Xu, J.H. Xu, Z.Y. Wu, Y.L. Wei and Z.P. Zhou. An *in situ* FTIR investigation on the adsorption of nitrosamines in zeolites. *Microporous Mesoporous Mater.*, **2004**, 72, 127-135.
- [23] S.L. Baum, I.G.M. Anderson, R.R. Baker, D.M. Murphy and C.C. Rowlands. Electron spin resonance and spin trap investigation of free radicals in cigarette smoke: development of a quantification procedure, *Analy. Chim. Acta*, **2003**, 481, 1-13.
- [24] F. Cunningham, M. Ghosh and M. Gaca, Applications of a Novel Method to Detect Particulate Phase Free Radical Generation from Cigarette Smoke using Electron Spin Resonance. The 13th Annual Meeting of Society of Free Radicals in Biology and Medicine, Denver, Colorado, **2006**, poster 251.
- [25] M. Ghosh, P. Ionita, J. McAughey and F. Cunningham, Electronic paramagnetic resonance investigation of the free radicals in gas and particulate phases of cigarette smoke using spin trapping techniques. *J. ARKIVOC*, **2008**, 12, 74-84.
- [26] D.F. Church, W.A. Pryor, Free-radical chemistry of cigarette smoke and its toxicological implications. *Environ. Health Perspectives*, **1985**, 64, 111-126.